Electronic Supplementary Material (ESI) for Physical Chemistry Chemical Physics.

SUPPORTING INFORMATION

Ab-initio prediction of structuring / mesoscale inhomogeneities in surfactant-free microemulsions and hydrogen-bonding-free microemulsions

Maximilian Hahn,[†,§] Sebastian Krickl,[†] Thomas Buchecker,[‡] Gasper Jost,[‡] Didier Touraud,[†] Pierre Bauduin,[¶] Arno Pfitzner,[‡] Andreas Klamt,[*,†,§] and Werner Kunz[*,†]

†*Institute of Physical and Theoretical Chemistry, University of Regensburg, 93040 Regensburg, Germany.*

‡*Institute of Inorganic Chemistry, University of Regensburg, 93040 Regensburg, Germany.*

¶ *Institut de chimie séparative de Marcoule (ICSM), UMR 5257 (CEA, CNRS, UM, ENSCM), BP 17171, 30207 Bagnols-sur-Cèze, France.*

§*COSMOlogic GmbH & Co. KG, Imbacher Weg 46, 51379 Leverkusen, Germany.*

E-mail: klamt@cosmologic.de; werner.kunz@chemie.uni-regensburg.de

COSMOplex results

Equivalence of the applied calculation set-ups

Several different calculation set-ups have been evaluated, differing by the composition of the phases in the simulation box and the orientation of the polarity moments of the self-organizing system (s.o.s.) phases. However, in case of strong convergence criteria being applied, the outcome of the COSMOplex calculations should be more or less equivalent. This is demonstrated by means of the COSMOplex results for acetoni-

trile/acetone/limonene at a phase composition of 0.30/0.35/0.35 in mole fractions (see figure 1) with the following calculation set-ups:

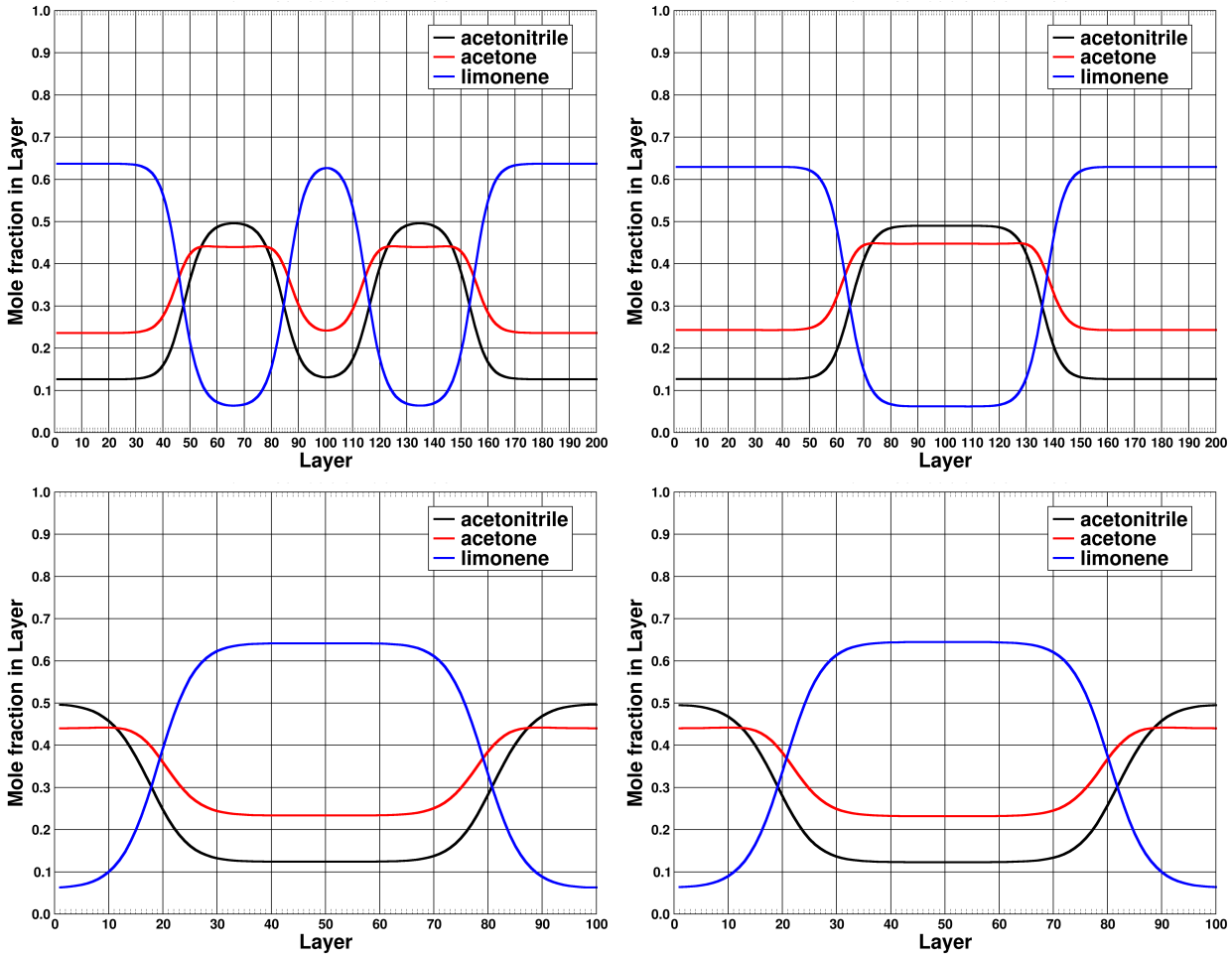

Figure 1: COSMOplex results for the HBFME system acetonitrile/acetone/limonene at a phase composition of 0.30/0.35/0.35 in mole fractions. Calculations performed on TZVPD-FINE level at a temperature of 25 °C with different calculation set-ups: (top left: bulk ← → bulk), (top right: bulk →← bulk), (bottom left: ←→←→←→←→) and (bottom right: bulk ←→←→←→ bulk) calculation set-up. Refined convergence thresholds – being 1000 times lower than the COSMOplex default values – were applied.

- mixture bulk phase (9 nm), s.o.s. phase (1 nm), s.o.s. phase (1 nm), mixture bulk phase (9 nm) – with symmetric polarity moments of the molecules in the s.o.s. phases: (bulk ← → bulk) or (bulk →← bulk) – see figure 1, top row.

- 8 s.o.s. phases (1.25 nm each) – with alternating polarity moments of the molecules

in the s.o.s. phases (←→←→←→←→) – see figure1, bottom left.

- mixture bulk phase (3.5 nm), 6 s.o.s. phases (0.5 nm each) with alternating polarity moments, mixture bulk phase (3.5 nm): (bulk ←→←→←→ bulk).we also learn that the hydrotropic component acetone shows a higher affinity towards acetonitrile than towards limonene – see figure1, bottom right.

Spontaneous microemulsion-like structuring

Within this contribution, we often stated that fluctuation period lengths of COSMOplex results are strongly influenced by the definition of the calculation set-up and specifically the number, length and orientation of s.o.s. phases in the simulation box and might not have a physical meaning. This is due to the fact that the molecules in the simulation box need to be pre-orientated in order to deflect the system from the homogeneous equilibrium state. As a result, the location and number of peaks in the performed COSMOplex simulations have their origin in the definition of the calculation set-up.

Nevertheless, it is possible to observe a spontaneous microemulsion-like structuring with the COSMOplex model in SFME systems. As prove of concept, this is illustrated for the water/THF/anisole system at a phase composition of 0.50/0.40/0.10 in mole fractions on the left-hand side of figure 2. However it needs to be emphasized again that the free energy differences in the formation of aggregate structures in the investigated systems are expected to be very small. Furthermore, the spontaneous formation of pronounced microemulsion-like structures in the evaluated system was only observed in close proximity to the COSMO-RS predicted LLE mixture critical point.

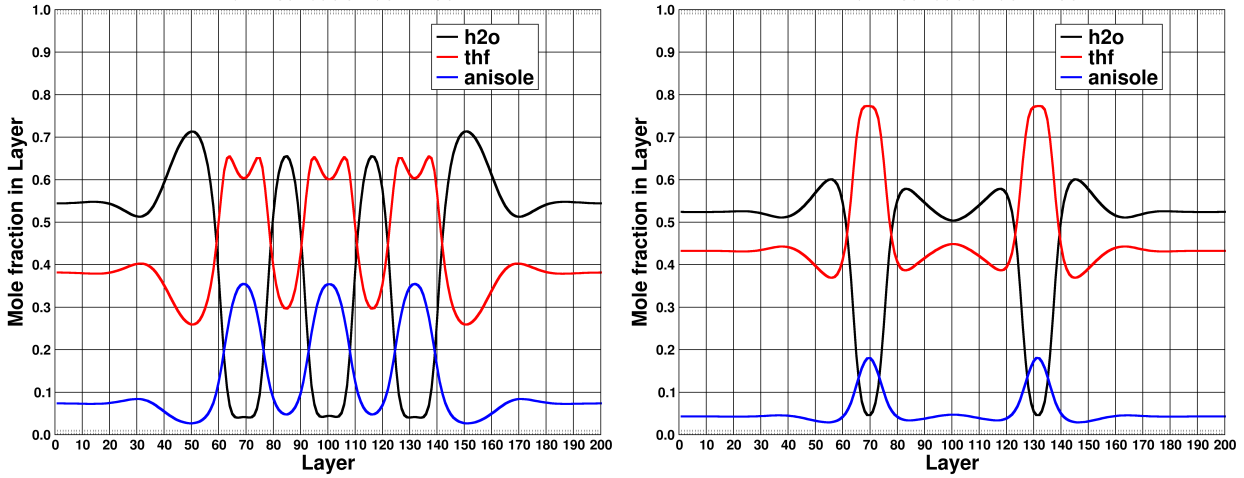

Figure 2: COSMOplex predicted fluctuations in water/THF/limonene at mole fraction phase compositions of 0.50/0.40/0.10 (left) and 0.50/0.45/0.05 (right) in mole fractions. From the amplitude heights of the predicted layer composition fluctuations, we learn that the structuring in proximity of the mixture critical point in the ternary phase diagram is significantly stronger. Calculations performed on TZVPD-FINE level at a temperature of 25 °C with (bulk ←→ bulk) calculation set-up. Refined convergence thresholds – being 100 times lower than the COSMOplex default values – were applied. Note the spontaneous microemulsion-like structuring at a phase composition of 0.50/0.40/0.10 (left) in mole fractions, and hence in close proximity to the LLE mixture critical point of the COSMO-RS predicted ternary phase diagram.

Choice of the proper COSMOplex calculation level for hydrogen-bonding-free systems

Comparing COSMOplex results for the acetonitrile/acetone/limonene system at different calculation levels (see figure 3 and figure 4: TZVP in the top rows vs. TZVPD-FINE in the bottom rows), we observed considerably higher fluctuation amplitudes – indicating a higher affinity of the molecules to aggregate – at the superior TZVPD-FINE level. This can be attributed to two features: the residual dielectric charge correction in the underlying COSMO-RS calculations and the better definition of hydrogen bonding between the interacting COSMO surface segments. In TZVP level calculations, a hydrogen bonding threshold is used and all COSMO surface segments with high enough polarization charge density are seen as potentially hydrogen bonding, while at TZVPD-FINE level, also the geometry of the molecule and the location and number of lone pairs are taken into account.

Both effects have reduced the contributions to the free energies arising from erroneously predicted hydrogen bonding in the HBFME system by several orders of magnitude.

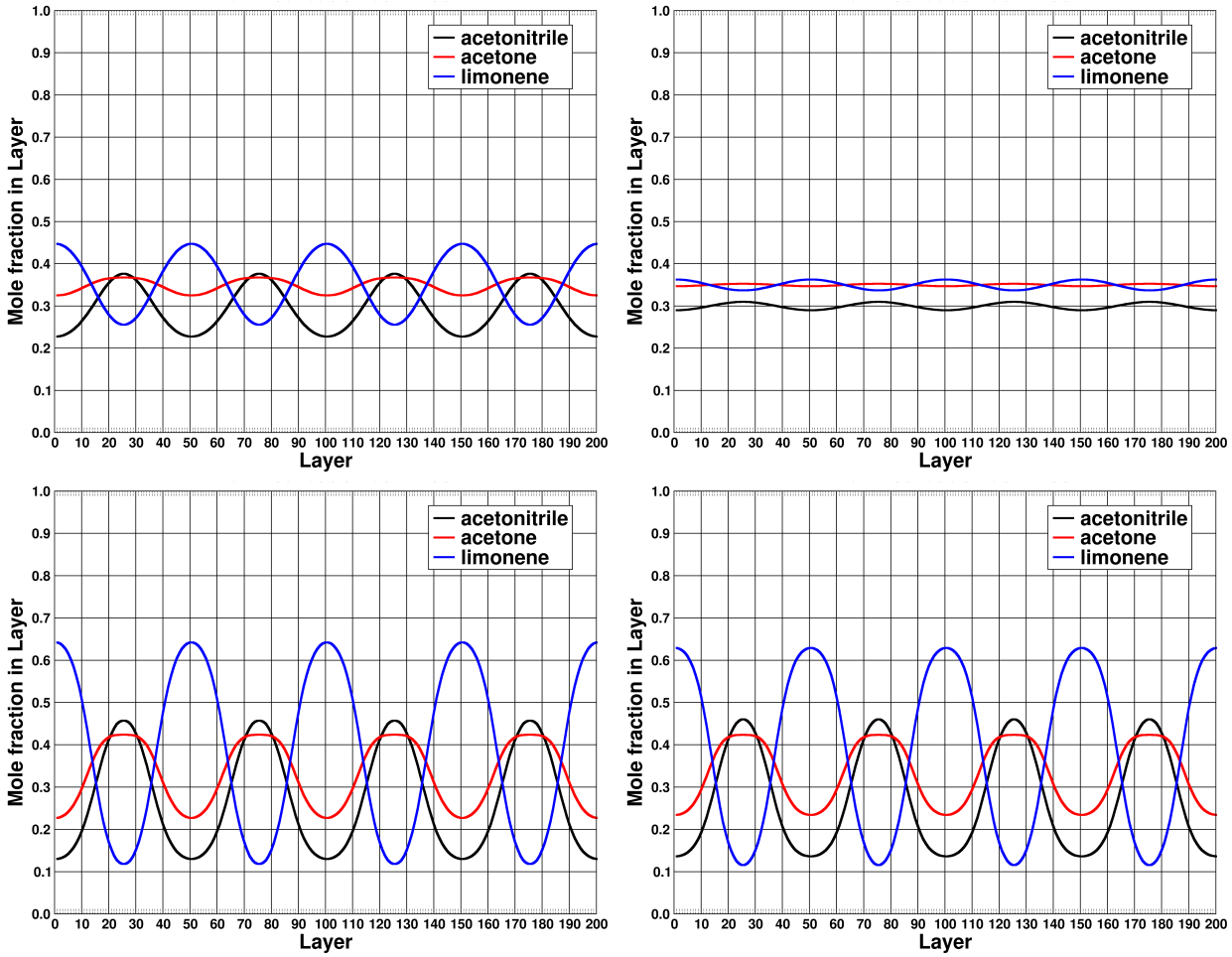

Figure 3: COSMOplex results for acetonitrile/acetone/limonene at a phase composition of 0.30/0.35/0.35 in mole fractions. Calculations performed on TZVP level (top row) and TZVPD-FINE level (bottom row) at a temperature of 25 °C with 8 s.o.s. phases and alternating polarity moments. Refined convergence thresholds – being 100 times (left-hand side) and 1000 times (right-hand side) lower than the COSMOplex default values – were applied.

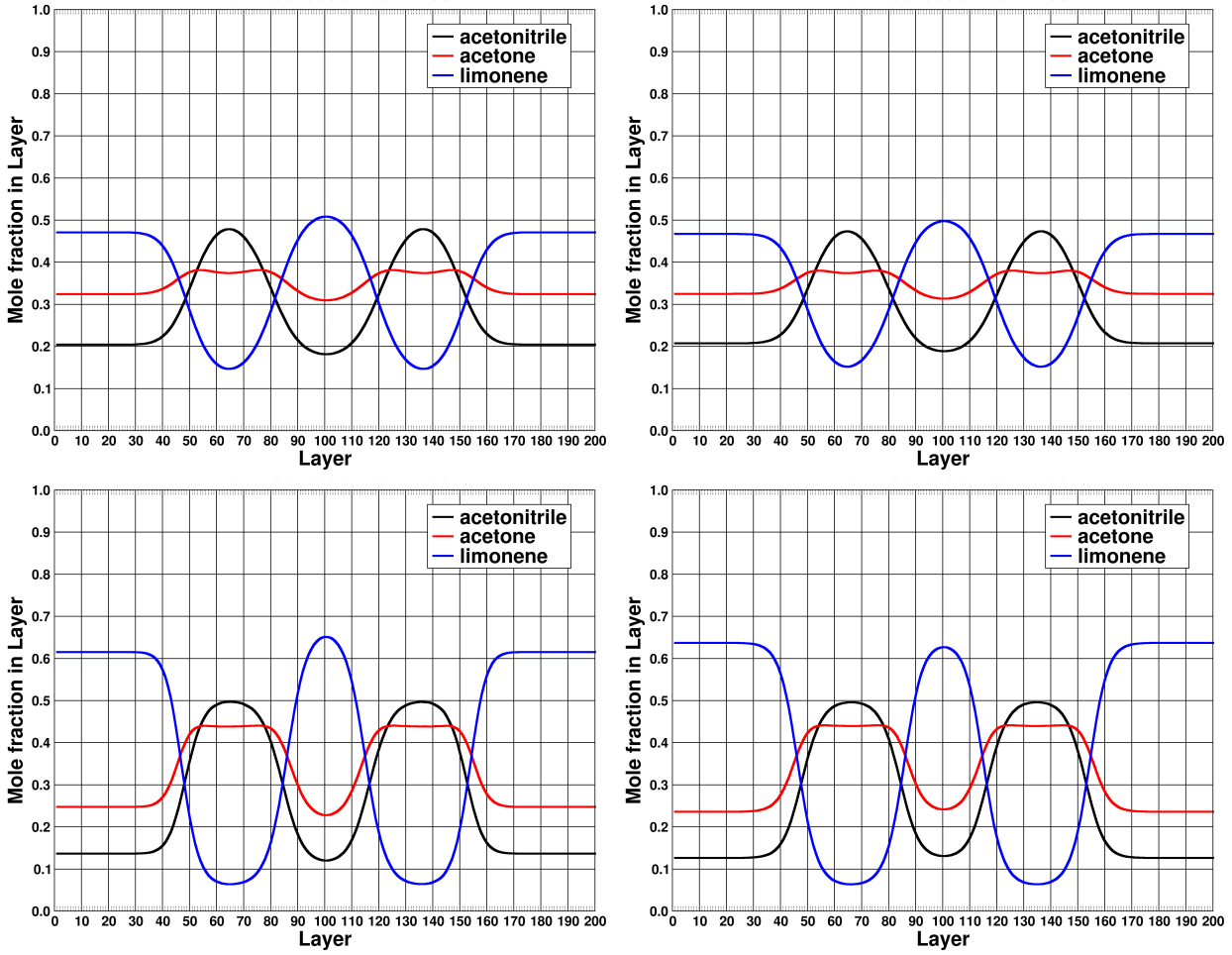

Figure 4: COSMOplex results for acetonitrile/acetone/limonene at a phase composition of 0.30/0.35/0.35 in mole fractions. Calculations performed on TZVP level (top row) and TZVPD-FINE level (bottom row) at a temperature of 25 °C with (bulk ← → bulk) calculation set-up. Refined convergence thresholds – being 100 times (left-hand side) and 1000 times (right-hand side) lower than the COSMOplex default values – were applied.

Simulation gradient as stability criterion

For simulations differing only in the applied convergence thresholds, the differences in the absolute fluctuation amplitude heights can be interpreted as a system, composition and temperature dependent simulation gradient. Within this contribution, we compare COSMOplex results obtained by use of two distinct sets of convergence thresholds – being 100 and 1000 times lower than the COSMOplex default values. The obtained results

indicate a correlation between this simulation gradient of COSMOplex calculations and the stability and reliability of the predicted structuring. The most stable structures with the lowest simulation gradients were observed at phase compositions corresponding to points located in proximity to the LLE miscibility gap in ternary phase diagrams.

For phase compositions far from the miscibility gap in ternary phase diagrams, a fast decaying of the predicted fluctuation amplitude heights with increasing number of COSMOplex iterations (due to stricter convergence criteria) was observed. The corresponding large negative simulation gradient indicates that the predicted fluctuations are relatively instable and will further decay and eventually vanish completely if the simulation is continued with stricter convergence criteria. In contrast to that, relatively stable fluctuations could be obtained for the evaluated SFME and HBFME systems at phase compositions corresponding to points in the pre-Ouzo region of the ternary phase diagrams. The results for the water/hydrotrope/anisole systems are depicted in the following figures: water/ethanol/anisole in figure 5, water/acetone/anisole in figure 6 and water/THF/anisole in figure 7. The results for the acetonitrile/acetone/limonene system are shown in figure 8.

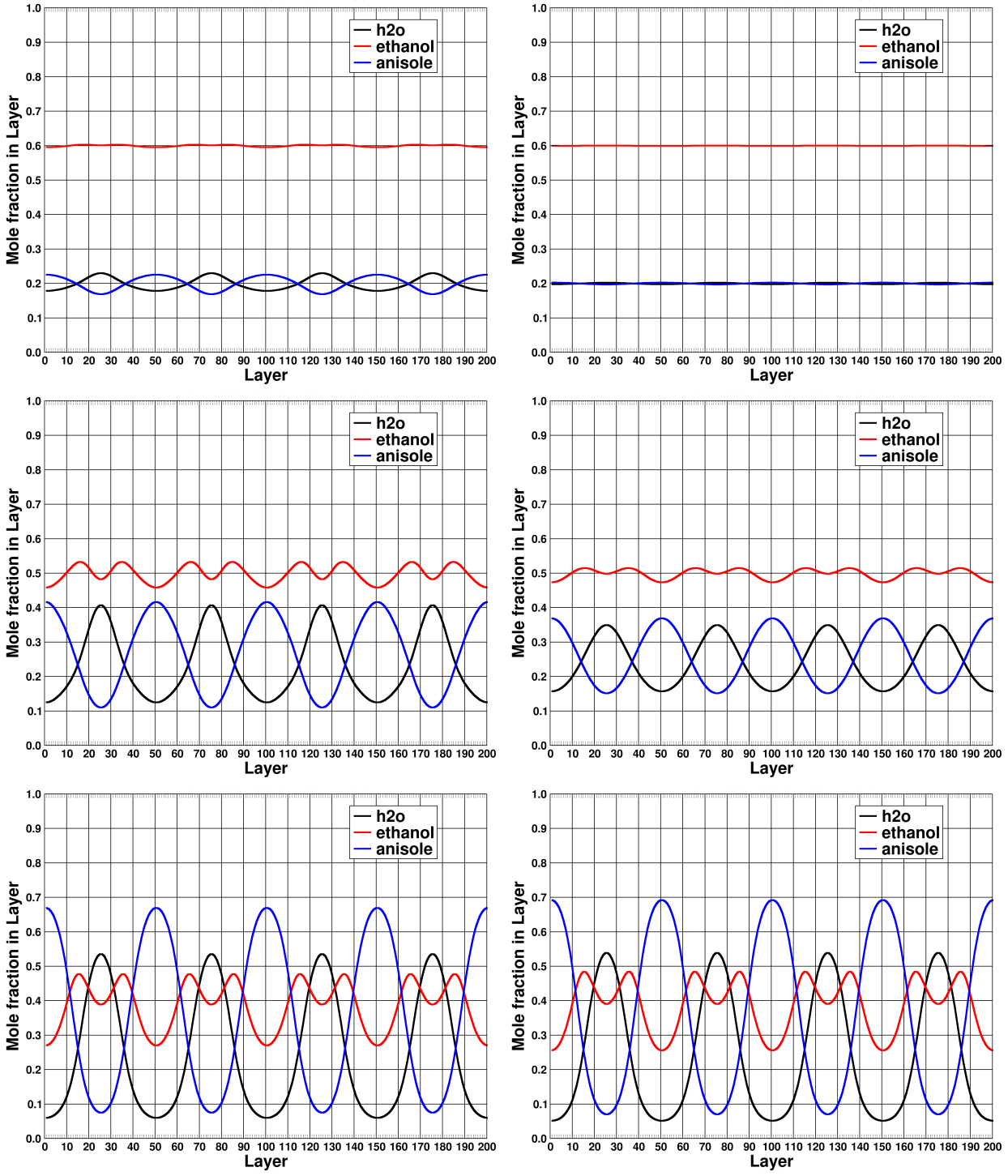

Figure 5: COSMOplex results for water/ethanol/anisole at phase compositions of 0.20/0.60/0.20 (top row), 0.25/0.50/0.25 (middle row), and 0.30/0.40/0.30 (bottom row) in mole fractions. Calculations performed on TZVPD-FINE level at a temperature of 25 °C with 8 s.o.s. phases and alternating polarity moments. Refined convergence thresholds were applied: 100 times lower (left-hand side) and 1000 times lower (right-hand side) than the COSMOplex default values.

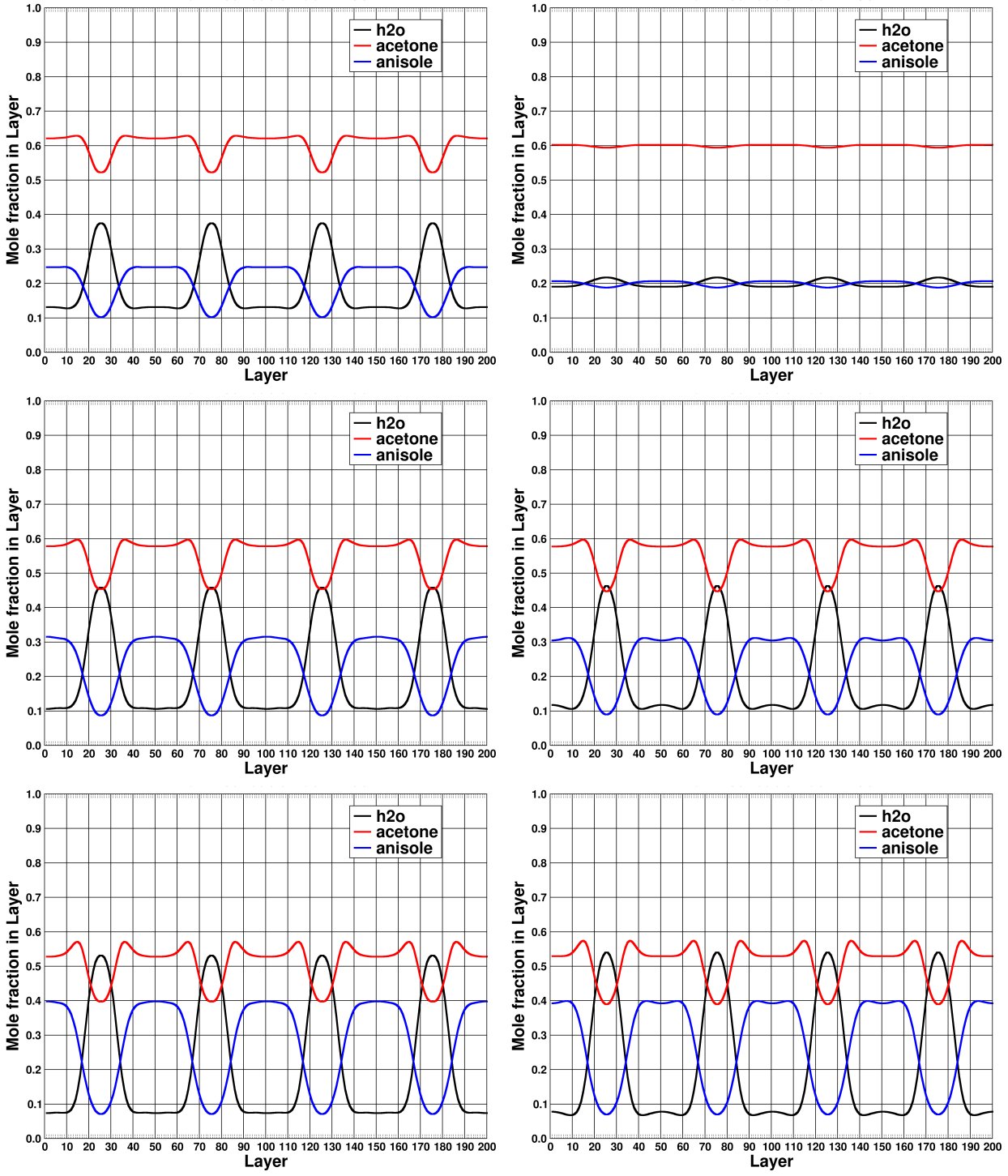

Figure 6: COSMOplex results for water/acetone/anisole at phase compositions of 0.20/0.60/0.20 (top row), 0.225/0.55/0.225 (middle row), and 0.25/0.50/0.25 (bottom row) in mole fractions. Calculations performed on TZVPD-FINE level at a temperature of 25 °C with 8 s.o.s. phases and alternating polarity moments. Refined convergence thresholds were applied: 100 times lower (left-hand side) and 1000 times lower (right-hand side) than the COSMOplex default values.

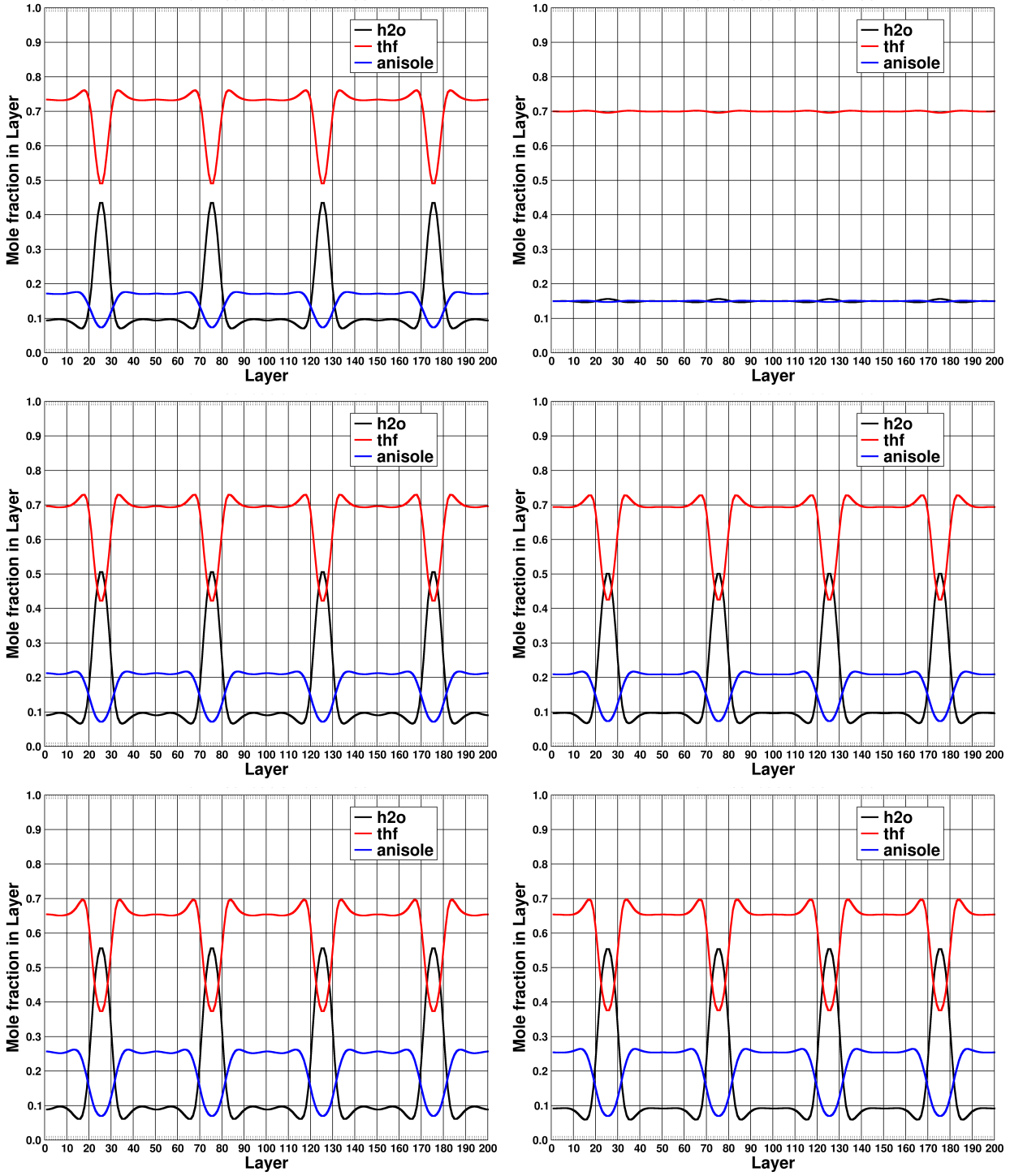

Figure 7: COSMOplex results for water/THF/anisole at phase compositions of 0.15/0.70/0.15 (top row), 0.175/0.65/0.175 (middle row), and 0.20/0.60/0.20 (bottom row) in mole fractions. Calculations performed on TZVPD-FINE level at a temperature of 25 °C with 8 s.o.s. phases and alternating polarity moments. Refined convergence thresholds were applied: 100 times lower (left-hand side) and 1000 times lower (right-hand side) than the COSMOplex default values.

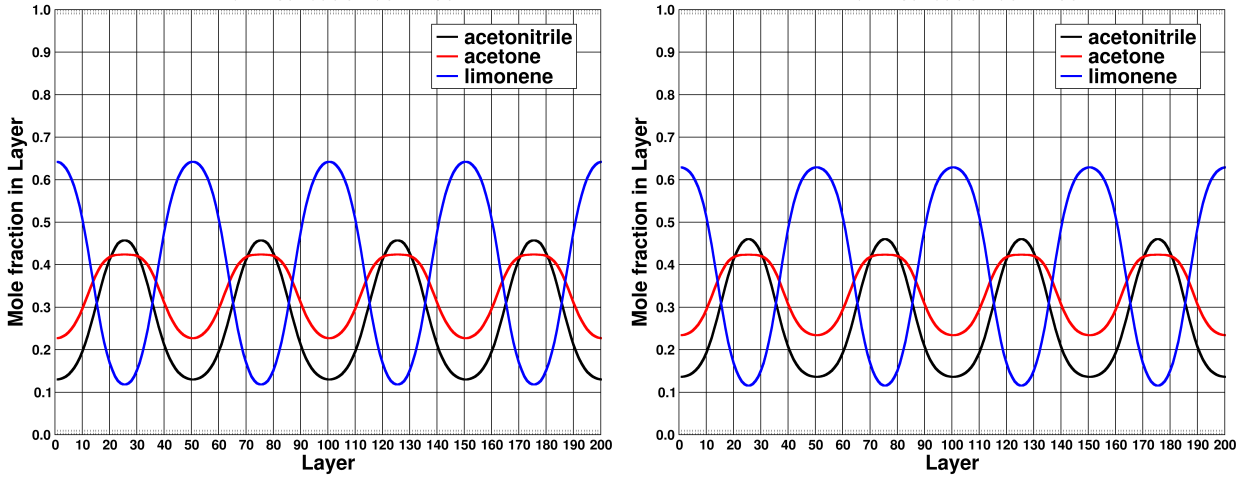

Figure 8: COSMOplex results for acetonitrile/acetone/limonene at phase compositions of 0.30/0.35/0.35 in mole fractions. Calculations performed on TZVPD-FINE level at a temperature of 25 °C with 8 s.o.s. phases and alternating polarity moments. Refined convergence thresholds were applied: 100 times lower (left-hand side) and 1000 times lower (right-hand side) than the COSMOplex default values.

Probability distribution curves and corresponding free energy differences

Within this contribution, the COSMOplex results are often shown in the form of layer composition curves, i.e. mole fraction vs layers plots. Although such representations of ternary systems are rather unusual, they have the big advantage that each layer can easily be mapped to a point in the ternary phase diagram. Furthermore, the layer composition curves are closely related to probability distribution curves showing the relative probability to find a molecule of a compound in a given COSMOplex simulation box layer plotted against the the depth (z-coordinate) of the COSMOplex simulation box.

The probability distribution curves for the acetonitrile/acetone/limonene and water/ethanol/-anisole systems at the evaluated phase compositions are given on the left-hand side of figures 9 and 10. The plots on the right-hand side of figures 9 and 10 show the free energy differences of the compounds in a given simulation box layer with respect to the free energy in the first simulation box layer plotted against the depth of the COSMOplex

simulation box. The corresponding layer composition curves are shown e.g. in figures 8 and 5, respectively.

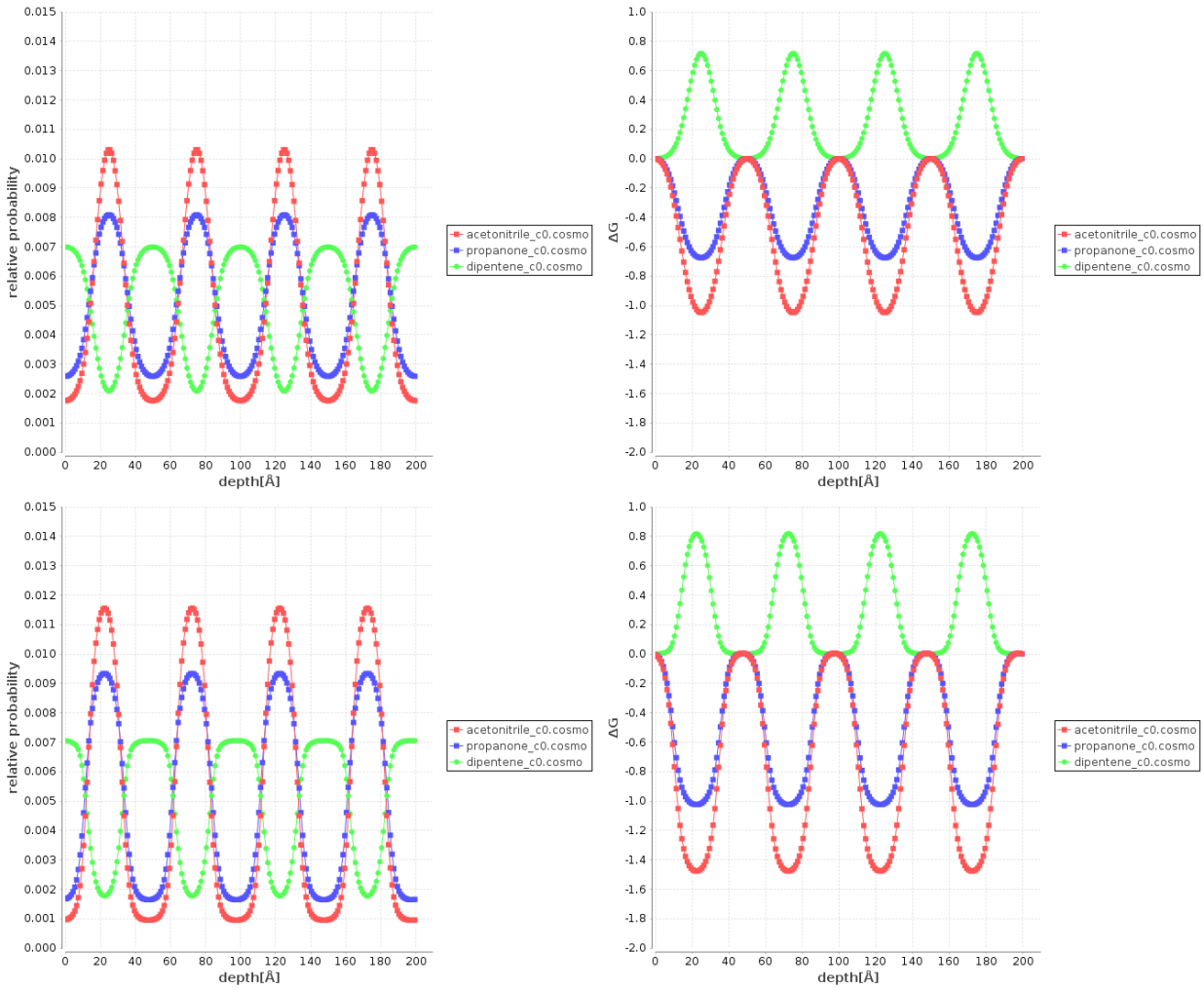

Figure 9: COSMOplex results for acetonitrile/acetone/limonene at phase compositions of 0.30/0.35/0.35 and 0.50/0.10/0.40 in mole fractions: probability distribution curves (left-hand side) and free energy difference curves (right-hand side). Calculations performed on TZVPD-FINE level at a temperature of 25 °C with 8 s.o.s. phases and alternating polarity moments. Refined convergence thresholds – being 100 times lower than the COSMOplex default values – were applied.

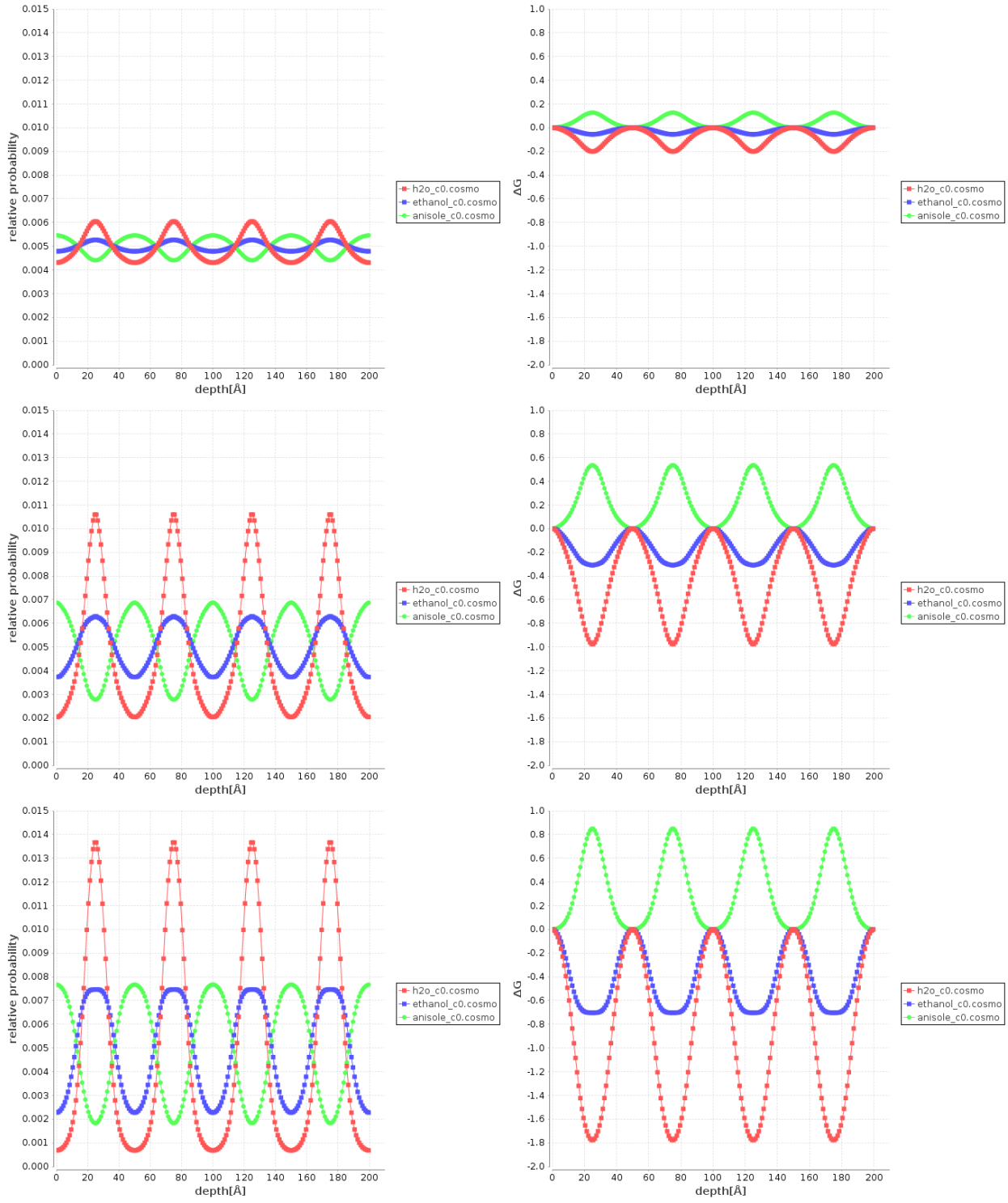

Figure 10: COSMOplex results for water/ethanol/anisole at phase compositions of 0.20/0.60/0.20 (top row), 0.25/0.50/0.25 (middle row), and 0.30/0.40/0.30 (bottom row) in mole fractions: probability distribution curves (left-hand side) and free energy difference curves (right-hand side). Calculations performed on TZVPD-FINE level at a temperature of 25 °C with 8 s.o.s. phases and alternating polarity moments. Refined convergence thresholds – being 100 times lower than the COSMOplex default values – were applied.

Figure 11 shows the COSMOplex predicted probability distribution and corresponding free energy difference curves for the ternary systems: water/ethanol/anisole (top row, phase composition: 0.25/0.50/0.25), water/acetone/anisole (middle row, phase composition: 0.20/0.60/0.20) and water/THF/anisole (bottom row, phase composition: 0.15/0.70/0.15). All calculations were performed on TZVPD-FINE level at a temperature of 25 °C with (bulk ←→←→←→ bulk) calculation set-up. Note that the COSMOplex results for the water/acetone/anisole and water/THF/anisole system indicate the formation of water-rich aggregates and relatively homogeneous, "bulk-like" compartments in the pre-Ouzo regions of the corresponding ternary phase diagrams, while the results for the water/ethanol/anisole system indicates a pronounced microemulsion-like structuring in the monophasic region of the SFME.

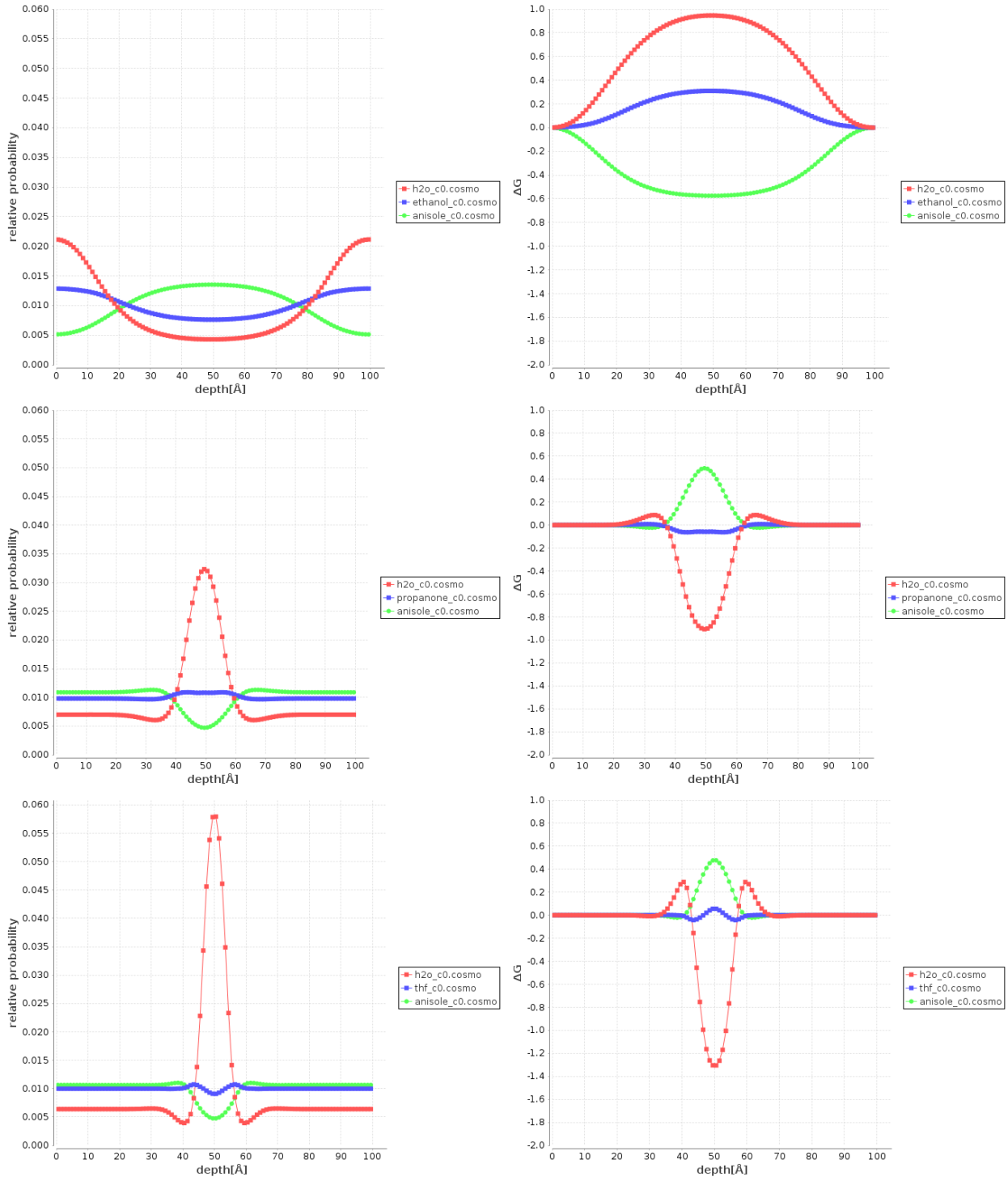

Figure 11: COSMOplex results for water/ethanol/anisole (top row, phase composition: 0.25/0.50/0.25), water/acetone/anisole (middle row, phase composition: 0.20/0.60/0.20) and water/THF/anisole (bottom row, phase composition: 0.15/0.70/0.15): probability distribution curves (left-hand side) and free energy difference curves (right-hand side). Calculations performed on TZVPD-FINE level at a temperature of 25 °C with (bulk ←→←→←→ bulk) calculation set-up. Refined convergence thresholds – being 1000 times lower than the COSMOplex default values – were applied.

Visualization of COSMOplex predicted composition fluctuations in ternary phase diagrams

Water/Hydrotrope/Anisole

The COSMOplex predicted composition fluctuations in the ternary phase diagrams of figure 12 correspond to the COSMOplex results depicted on the right-hand sides of figures 5 (water/ethanol/anisole), 6 (water/acetone/anisole) and 7 (water/THF/anisole), respectively. All COSMO-RS and COSMOplex calculations were performed on TZVPD-FINE level at a temperature of 25 °C. 8 s.o.s. phases and alternating polarity moments were used for the COSMOplex calculation set-up and convergence thresholds – being 1000 times lower than the COSMOplex default values – were applied.

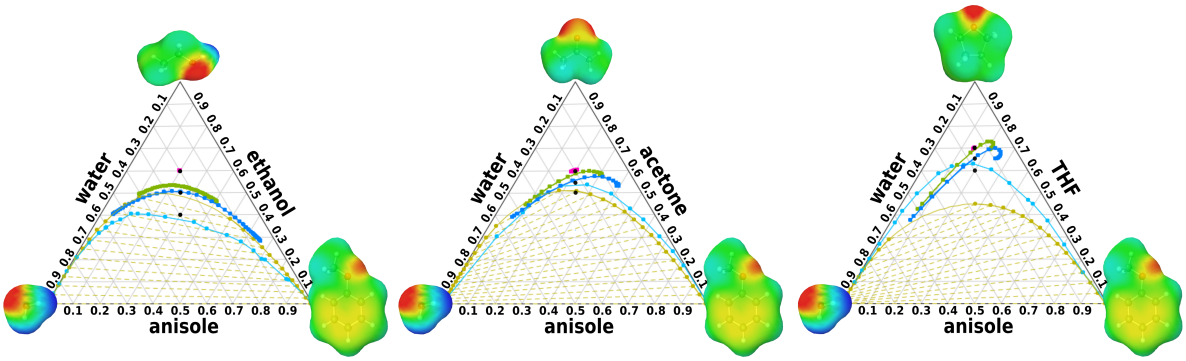

Figure 12: Ternary phase diagrams (flat blue: experiment, flat green: predicted with COSMO-RS) of water/ethanol/anisole (left), water/acetone/anisole (middle) and water/THF/anisole (right) – including COSMOplex-predicted fluctuations around the overall mole fraction phase compositions, which are indicated by the black dots in the ternary phase diagrams.

Compound and system free energies of aggregation and self-organization in water/hydrotrope/anisole mixtures

Mean values for the COSMOplex predicted compound and system free energies of aggregation and self-organization of the molecules in water/ethanol/anisole, water/acetone/anisole

and water/THF/anisole at given phase compositions are compiled in table 1. Note that the amplitude heights of COSMOplex predicted free energy fluctuations (indicated by the rmsd values in the last column of table 1) – which are due to the inhomogeneities in the layer compositions within the simulation box – are in good correlation with the corresponding relative amplitude heights of the COSMOplex predicted fluctuations (shown e.g. on the left-hand sides of figures 5, 6 and 7).

Table 1: Mean compound and system free energies of aggregation and self-organization in water/hydrotrope/anisole at 25 °C (with ethanol, acetone and THF as hydrotropic compound). The mean system free energies $\Delta G^0_{s.o.s.}$ and $\Delta G_{s.o.s.}$ are mole fraction weighted sums of the mean compound free energy differences of aggregation and self-organization with and without contributions arising from the pressure function and the electrostatic potential, respectively. The amplitude heights of free energy fluctuations ($h_{fluct.}(\Delta G_{s.o.s.})$) corresponding to $\Delta G_{s.o.s.}$ are indicated by their rmsd values in the last column. All energy values are given in the unit kcal/mol and correspond to COSMOplex calculations on TZVPD-FINE level with (←→←→←→←→) calculation set-up and refined convergence thresholds (100 times lower than the COSMOplex default values).

phase composition	mean compound free energies			system free energy		
	compound 1	*compound* 2	*compound* 3	$\Delta G^0_{s.o.s.}$	$\Delta G_{s.o.s.}$	$h_{fluct.}(\Delta G_{s.o.s.})$
	water	*ethanol*	*anisole*			
0.10/0.80/0.10	0.10079	−0.03678	−0.10112	−0.02945	−0.02952	±0.00254
0.15/0.70/0.15	0.10714	−0.04254	−0.09567	−0.02805	−0.02806	±0.00591
0.20/0.60/0.20	0.09783	−0.04605	−0.09221	−0.02651	−0.02653	±0.01780
0.25/0.50/0.25	0.04351	−0.01417	−0.10199	−0.02171	−0.02220	±0.10093
0.30/0.40/0.30	−0.03839	0.05145	−0.11158	−0.02441	−0.02492	±0.23983
	water	*acetone*	*anisole*			
0.10/0.80/0.10	0.15734	−0.05632	−0.09089	−0.03841	−0.05277	±0.01553
0.15/0.70/0.15	0.16080	−0.06966	−0.09617	−0.03907	−0.04990	±0.01505
0.20/0.60/0.20	0.10202	−0.05848	−0.10238	−0.03516	−0.04264	±0.04575
0.25/0.50/0.25	0.01490	−0.00849	−0.11974	−0.03046	−0.03606	±0.10826
0.30/0.40/0.30	−0.07063	0.06594	−0.12698	−0.03290	−0.03693	±0.19377
	water	*THF*	*anisole*			
0.10/0.80/0.10	0.30618	−0.08457	−0.04524	−0.04156	−0.04211	±0.00665
0.15/0.70/0.15	0.19769	−0.08060	−0.05510	−0.03503	−0.03759	±0.04007
0.20/0.60/0.20	0.13930	−0.07794	−0.06498	−0.03189	−0.03440	±0.05905
0.25/0.50/0.25	0.07914	−0.05518	−0.07532	−0.02664	−0.02889	±0.09310
0.30/0.40/0.30	−0.00506	0.00607	−0.07422	−0.02135	−0.02406	±0.14516

Results also indicate that the aggregation of hydrotrope and anisole molecules can be seen as the driving force for the observed microemulsion-like structuring in the pre-Ouzo region of the SFME systems. However, with decreasing hydrotrope content and increasing water and anisole content, a shift of the compound free energies of aggregation and self-organization of the compounds water and anisole towards lower values can be observed, indicating a higher affinity to form aggregate structures. At a phase composition of 0.30/0.40/0.30 in mole fractions, the stabilizing effect of the hydrotrope molecules is lost and the self-aggregation of the immiscible components water and anisole is the driving force for aggregation, or more precisely, for the phase separation. Hence, the results are in good agreement with the location of the COSMO-RS predicted LLE-miscibility gap in the ternary water/ethanol/anisole and water/THF/anisole phase diagrams. Please note that the COSMOplex predicted free energy values compiled in table 1 are dependent on the applied convergence criteria and the reasonable definition of the calculation parameters. In case of the water/acetone/anisole system, we were able to find the same good correlation with the location of the miscibility gap by applying stricter convergence criteria (convergence thresholds being 1000 times lower than the COSMOplex default values).

Solvation and hydrotropic efficiencies from a theoretical point of view

In order to evaluate and explain the hydrotropic strength of amphiphilic molecules, it is helpful to look upon solvation from a theoretical point of view. Let us consider liquid water at low temperatures as more or less ordered three-dimensional network, in which each molecule can form up to four hydrogen bonds to tetrahedrally coordinated neighbor molecules. Be aware that the formation of hydrogen bonds between two molecules and especially the formation of cooperative hydrogen bonds in a 3D network goes along with a tremendous loss of configurational entropy and strongly reduces the solubilizing power of a polar protic solvent. This is due to the fact that strongly interacting hydrogen bonds

have to be broken before a cavity for a solute molecule can form.

Then the question arises why non-polar molecules can be solvated by water after all. Curiously, the answer is again hydrogen bonding or more exactly the high degree of order in the solvation/hydration shells closest to the solute molecules. Due to the strong interactions via hydrogen bonds, positively charged molecular surfaces are most likely in contact with negatively charged molecular surfaces. The polar and oppositely charged molecular surfaces of the water molecules therefore tend to screen themselves and the resulting combined surface of a cluster of interacting water molecules is relatively non-polar. This behavior of water to be highly ordered in the first solvation shells is commonly known and can for instance be found in methane hydrates (methane ice), where a small methane molecule is encapsulated by highly ordered water molecules and forms clathrates. Liquid water is of course not that ordered but will still screen itself to a high degree and can therefore form cavities with low polarity. These principles are illustrated in fig. 13 with geometry optimized clusters of water molecules, screened by a virtual conductor with infinite dielectric (COSMO cavity).

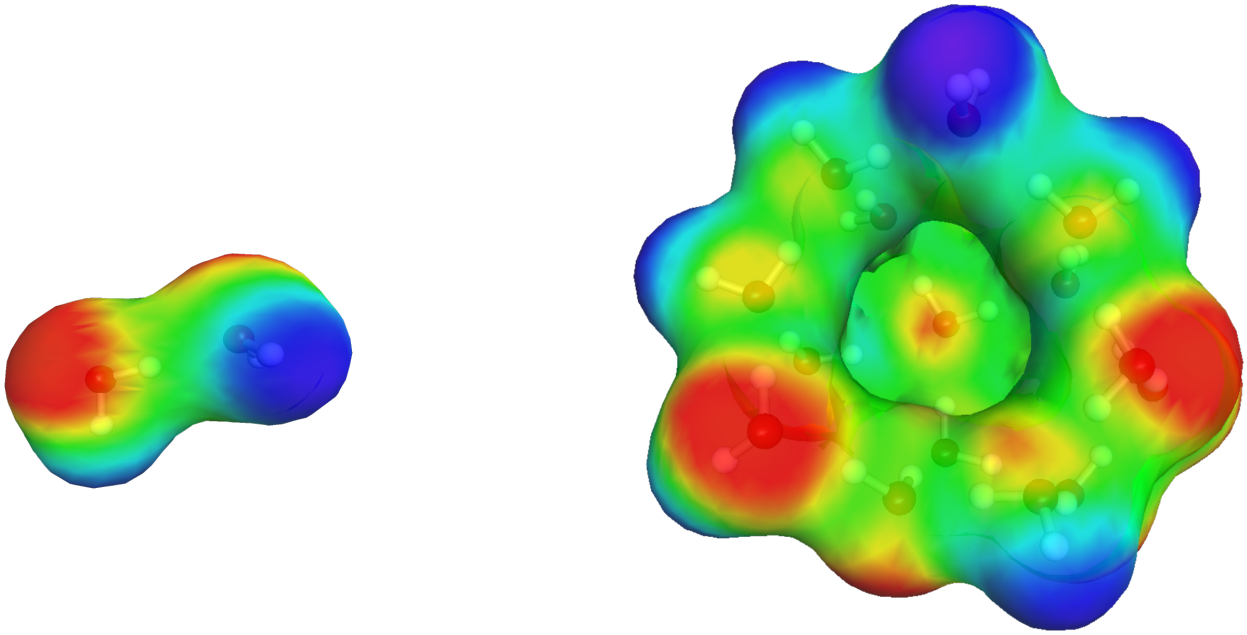

Figure 13: COSMO surfaces – color coded by polarization charge densities – of two interacting water molecules (left) and 15 interacting water molecules (right) screened by a virtual conductor. Geometry optimized with DFT-BP86/COSMO calculations using TURBOMOLE and TZVPD basis set. Polar and oppositely charged COSMO surfaces (deep blue and red) screen each other. The resulting clusters show more non-polar (green) COSMO surface area than the separated molecules.

The hydrogen bond induced degree of order in liquid water strongly depends on the temperature of the system and provides a good explanation for e.g. the density anomaly of liquid water. Furthermore, the formation of clusters of water molecules, interacting via hydrogen bonds, can be seen as the source of the hydrophobic behavior of non-polar solvents like e.g. heptane or toluene when mixed with water. From the σ-potentials of the evaluated solvents, it is evident that the solvation of hydrotrope molecules in non-polar solvents (like e.g. heptane or toluene) is only possible for entropic reasons, while in case of more polar solvents also a temperature dependent enthalpic contribution must be considered.

In order to enable the mixing of water with non-polar solvents, or more general of water-rich with oil-rich phases, hydrotropes can be used as solubilizers. Due to their amphiphilic

character, these molecules are likely to be miscible with both phases and therefore able to introduce and provide non-polar molecular surfaces in the water-rich and/or polar molecular surfaces in the oil-rich phase. However, due to the fact that most hydrotrope molecules provide much more non-polar molecular surface area than highly polar surface area, the first (introducing non-polar molecular surfaces into the water-rich phase) will have a higher influence on the solubilisation efficiency of the hydrotrope, indicated by the miscibility gap in the measured ternary phase diagrams.

Within the ternary water/hydrotrope/anisole systems evaluated within this study, the solubilizing power of the hydrotropic components can be correlated with the affinity of the hydrotropic compound in infinite dilution towards the water-rich phase and the amount of non-polar molecular surface of the corresponding hydrotrope. The first can be quantified either by infinite dilution activity coefficients or the partition coefficients of hydrotrope molecules in infinite dilution between the phases in a binary water-oil phase equilibrium, the second can be obtained from the σ-profiles of the hydrotrope molecules. The σ-profiles shown in figure 14, provide a detailed description of molecular polarity properties and can hence be used to quantify molecular interactions in solution. The σ-regions beyond ± 1 e/nm^2 must be considered as strongly polar and potentially hydrogen bonding, while the rest corresponds to weakly polar or non-polar surface areas. Note that the area under a σ-profile curve corresponds to the molecular surface of the molecule.

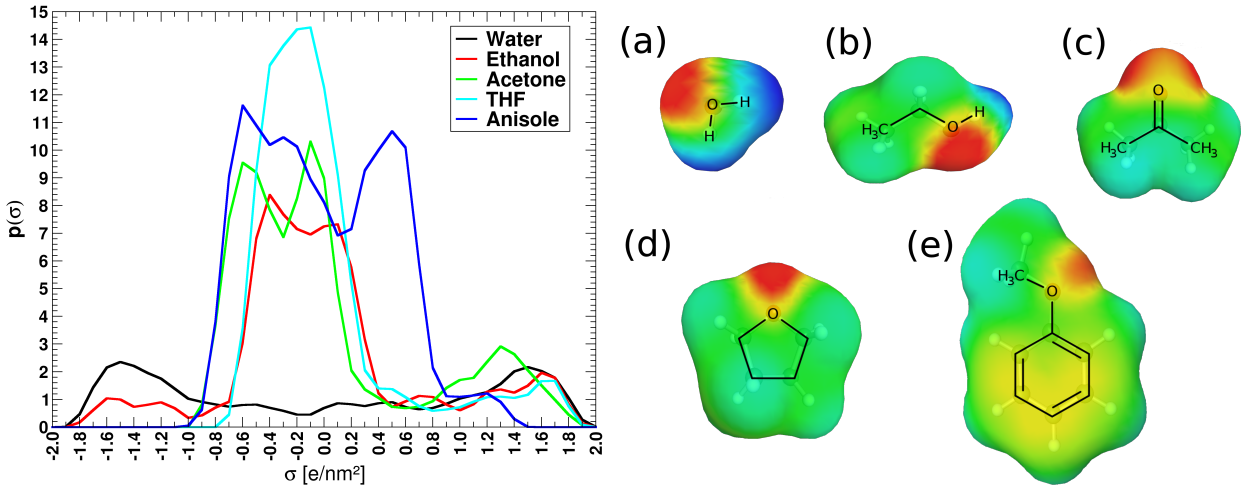

Figure 14: σ-profiles and corresponding COSMO surfaces of water, ethanol, acetone, tetrahydrofuran (THF) and anisole. The given σ-profiles provide a detailed description of molecular polarity properties and indicate the total area of COSMO surface with a specific polarity. The σ-regions beyond ± 1 e/nm^2 must be considered as stongly polar and potentially hydrogen bonding, while the rest corresponds to weakly polar or non-polar surface areas. For simplicity only one conformer is plotted for each molecule.

From the left side of fig. 14, it is obvious that the main difference between the hydrotrope molecules ethanol, acetone and THF can be found in the strongly polar σ-regions beyond ± 1 e/nm^2. This can be correlated to the availability of hydrogen bond donor and acceptor sites on the molecular surface of the hydrotrope molecules. Assuming that all correlation effects arising from the geometry of the molecules can be neglected in the first order, an optimal combination of the pairwise interacting COSMO surface segments in a liquid system should screen itself and consequently produce as less electrostatic misfit as possible. In other words, surface area with a specific polarity σ would preferably interact with surface area of polarity $-\sigma$. The corresponding combined σ-profile would be perfectly symmetric and the residual misfit charge would be zero.

Considering pure anisole, an optimal pairing of all COSMO surface segments is not possible, since the surface charge of the polar molecular surface corresponding to the oxygen atom of the anisole molecule can not be screened by other polar surfaces. However, as indicated by the σ-profiles in figure 14, the resulting residual misfit of anisole can be

reduced by adding ethanol molecules.

Beside of the obvious differences in the σ-regions beyond ± 1 e/nm^2, the hydrotropic molecules also differ to a high extent in the amount of non-polar and weakly polar surface area. From the σ-profiles we guess that from the three compounds, ethanol will show the highest and THF the lowest affinity towards water molecules. Infinite dilution partition coefficients between the phases in a binary water/anisole phase equilibrium at standard conditions confirm this trend. The results for the hydrotropes ethanol, acetone and THF are composed in table 2 (calculations performed with COSMOtherm, Version 18). Note that the values of the partition coefficient are given in decimal logarithmic units, whereby negative values indicate that the solute prefers the water-rich phase.

Table 2: Partition coefficients of the hydrotropes ethanol, acetone and THF in infinite dilution between the water-rich and oil-rich phases of binary water/oil mixtures at a temperature of 25 °C and corresponding phase compositions in mole fractions.

System :	*Solute* : *ethanol*	*Solute* : *acetone*	*Solute* : *THF*	*Phase*1	*Phase*2
water − *anisole*	−1.0041	−0.1497	0.4034	$x(h_2o) = 0.999747$ $x(anisole) = 0.000253$	$x(h_2o) = 0.006024$ $x(anisole) = 0.993976$
water − *THF*			0.4355	$x(h_2o) = 1.0$	$x(THF) = 1.0$
water − *acetone*		0.0855		$x(h_2o) = 1.0$	$x(acetone) = 1.0$
water − *ethanol*	0.1873			$x(h_2o) = 1.0$	$x(ethanol) = 1.0$